ELSEVIER

Nuclear Instruments and Methods in Physics Research A 465 (2001) 550–565

NUCLEAR INSTRUMENTS & METHODS IN PHYSICS RESEARCH Section A

www.elsevier.nl/locate/nima

The electronics and data acquisition systems of a CsI(Tl) scintillating crystal detector for low energy neutrino experiment

W.P. Lai[a,b], K.C. Cheng[a], H.B. Li[a,c], H.Y. Sheng[a,d], B.A. Zhuang[a,d], C.Y. Chang[e], C.P. Chen[a], Y.P. Chen[a], H.C. Hsu[a], J. Li[d], C.Y. Liang[f], Y. Liu[d], Z.S. Liu[g], C.S. Luo[a], F. Shi[d], R.F. Su[h], P.K. Teng[a], P.L. Wang[d], H.T. Wong[a,*], Z.Y. Zhang[g], D.X. Zhao[a,d], J.W. Zhao[d], P.P. Zhao[d], Z.Y. Zhou[i]

[a] *Institute of Physics, Academia Sinica, Taipei, Taiwan*
[b] *Department of Management Information Systems, Chung Kuo Institute of Technology, Taipei, Taiwan*
[c] *Department of Physics, National Taiwan University, Taipei, Taiwan*
[d] *Institute of High Energy Physics, Beijing, China*
[e] *Department of Physics, University of Maryland, College Park, USA*
[f] *Center of Material Science, National Tsing Hua University, Hsinchu, Taiwan*
[g] *Department of Electronics, Institute of Radiation Protection, Taiyuan, China*
[h] *Nuclear Engineering Division, Kuo-sheng Nuclear Power Station, Taiwan Power Company, Taiwan*
[i] *Department of Nuclear Physics, Institute of Atomic Energy, Beijing, China*

The TEXONO[1] collaboration

Received 23 October 2000; received in revised form 11 December 2000; accepted 15 December 2000

Abstract

A 500 kg CsI(Tl) scintillating crystal detector is under construction for the studies of low-energy neutrino physics. The requirements, design, realization and the performance of the associated electronics, trigger, data acquisition and software control systems are described. Possibilities for future extensions are discussed.

PACS: 29.40.Mc; 07.50.Qx; 07.05.M

Keywords: Scintillation detectors; Electronics; Data acquisition

1. Introduction

One of the major directions and experimental challenges in neutrino and astro-particle physics [1] is to extend the measurement capabilities to the

*Corresponding author. Tel.: +886-2-2789-9682; fax: +886-2-2788-9828.

E-mail address: htwong@phys.sinica.edu.tw (H.T. Wong).

[1] Taiwan EXperiment On NeutrinO.

0168-9002/01/$ - see front matter
PII: S0168-9002(01)00646-5

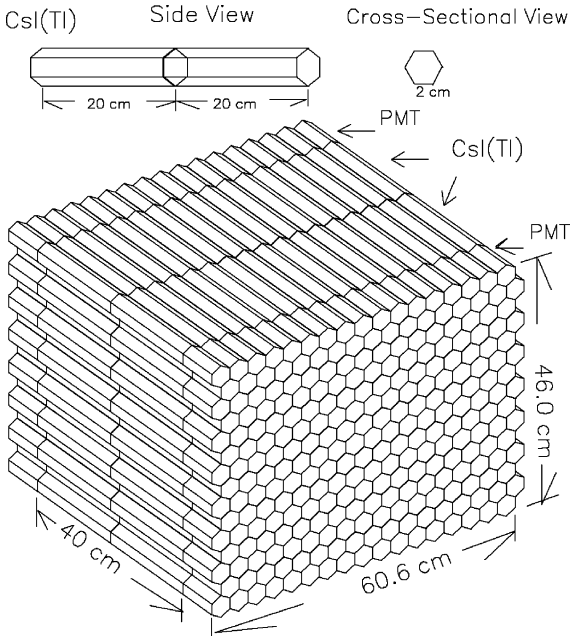

Fig. 1. Schematic drawings of the CsI(Tl) target configuration, showing a 2 (width) × 17 (depth) × 15 (height) matrix. Each individual crystal module is 20 cm long with a hexagonal cross-section of 2 cm edge. Readout is performed by photo-multipliers at both ends.

sub-MeV range for the detection of the p–p and ^{7}Be solar neutrinos, as well as for the searches of Weakly Interacting Massive Particles (WIMPs) and other topics. The merits of scintillating crystal detector in low-energy low-background experiment were recently discussed [2]. An experiment with a CsI(Tl) detector placed near a reactor core to study neutrino interactions at low energy is being constructed [3]. In the first data-taking phase, the detector is based on 200 kg of CsI(Tl) scintillating crystals[2] [4] read out by 200 photo-multipliers (PMTs)[3] made of special low-activity glass. The detector set-up is shown schematically in Fig. 1. The eventual goal will be to operate with 500 kg of CsI(Tl) crystals at the reactor. A Dark Matter-WIMP search experiment based on CsI(Tl) crystal as target at an underground laboratory is being planned.

[2] Manufacturer: Unique Crystals, Beijing.

[3] Hamamatsu CR110-10.

The sum of the two PMT signals for each crystal module gives the energy while their difference provides the longitudinal position information. The intrinsic rise and decay times for the emissions from CsI(Tl) are typically in the range of 100 ns and 2 μs, respectively. A typical signal from a ^{137}Cs source (γ-energy of 662 keV), as recorded by a 100 MHz digital oscilloscope, is shown in Fig. 2(a).

As depicted in Fig. 3, the detector assembly will be taking data inside an elaborate shielding structure consisting of, from inside out, layers of copper, boron-loaded polyethylene, steel and lead. On the outermost layer of the shielding are a total of 16 plastic scintillator panels each viewed by two 5 in PMTs. They provide veto signals for events induced by the traversing cosmic-rays.

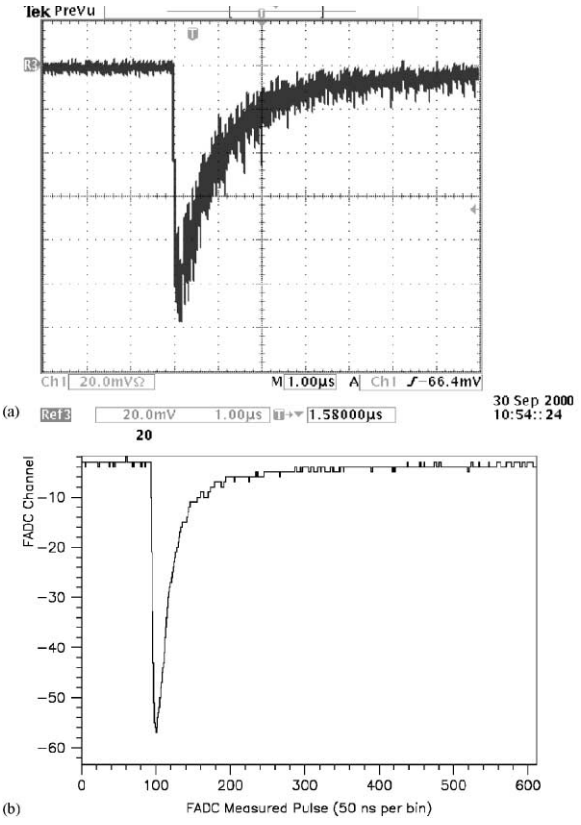

Fig. 2. (a) Raw input signal from CsI(Tl) + PMT as recorded by a 100 MHz digital oscilloscope. Time axis: 1 μs per division. (b) Output signal after shaping from the Amplifier-Shaper as recorded by the FADC. Time axis: 5 μs per 100 FADC time bin.

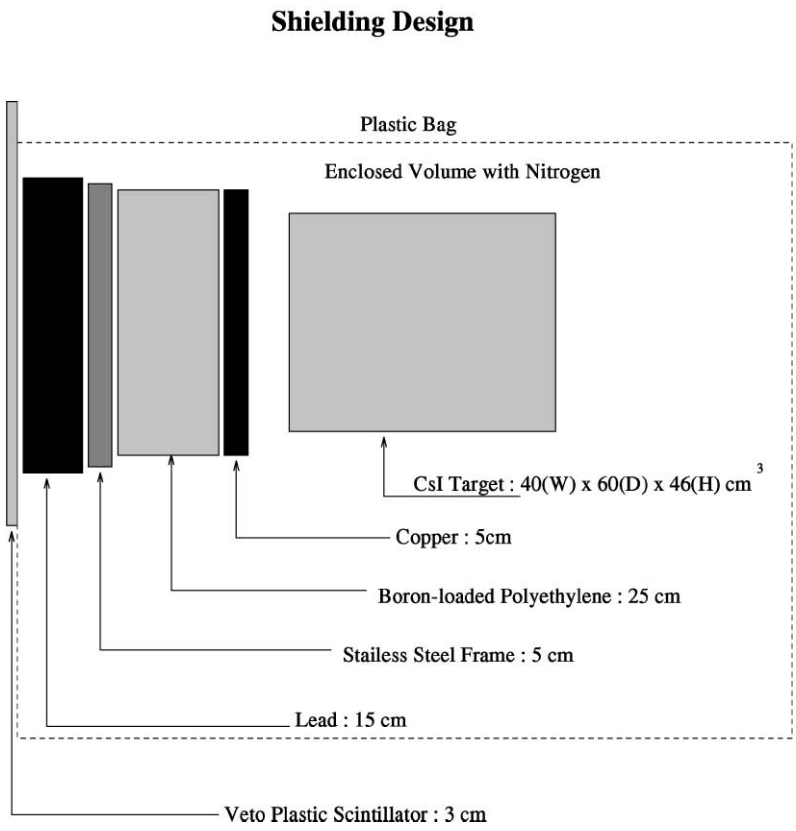

Fig. 3. Schematic diagram of the shielding configuration. The coverage is 4π but only one face is shown. There are a total of 16 plastic scintillator panels for cosmic-ray veto, each viewed by two photo-multipliers.

This article describes the requirements, design, construction and performance of the electronics, data acquisition (DAQ), and software control systems of this experiment. The basic design and parameters are applicable to similar class of experiments.

2. Requirements

The tasks and generic requirements to the electronics and data acquisition systems for this class of low-energy neutrino experiments are as follows:

1. Low detection threshold and yet a large dynamic range; the interesting signals for some applications can be as low as the range of 10 keV, while calibrations and background diagnostic studies would require the measurement of the minimum ionizing pulses from cosmic-ray muons, typically around 20–30 MeV.
2. Good energy response; crystal scintillators, with their higher light yield and more efficient light collection, typically provide better energy resolution than plastic and liquid scintillators. The readout electronics should exploit these advantages by providing good and linear energy response.
3. Complete record of relative timing; some signals and background channels are characterized by their timing correlations, especially within the 1 ms range. The readout system should be able to provide a timing sequence measurement as completely as possible.

4. Measurement of the pulse shape; events due to α-particles give different pulse shape in some scintillating crystals (such as NaI(Tl) and CsI(Tl)) to those due to electrons and photons [5]. Pulse shape information will allow discrimination between different categories of events.
5. Operation in non-optimal conditions; these class of experiments typically require data taking in underground laboratories or other remote sites, often without immediate equipment back-up support. The electronics and data acquisition systems should be able to operate automatically and reliably under such conditions.

As illustrations, in the measurement of $\bar{\nu}_e$-electron scatterings to study neutrino magnetic moments with reactor neutrinos [6] using crystal scintillators, the goal is to push the energy threshold for the recoil electrons as low as possible to the range of 10 keV [4]. The experimental signature is a single-hit out of the many channels, without a cosmic-veto signal and without any time-correlated background events. On the background side, the ^{214}Bi–^{214}Po decay sequence within the ^{238}U series provides a distinct $\beta-\alpha$ time-correlated signature which serve to identify the background event and to measure its contributions:

$$^{214}\mathrm{Bi} \rightarrow ^{214}\mathrm{Po} + \bar{\nu}_e + e^- + \gamma's$$
$$(Q = 3.28\ \mathrm{MeV};\ T_{1/2} = 19.8\ \mathrm{min})$$

$$^{214}\mathrm{Po} \rightarrow ^{210}\mathrm{Pb} + \alpha$$
$$(Q = 7.69\ \mathrm{MeV};\ T_{1/2} = 164\ \mu\mathrm{s}).$$

The identification of such cascade-events would require a time-sequence record and an α-tag at the specific energy for the second events. There are similar examples in the ^{232}Th and ^{235}U decay series as well.

3. Electronics system

The schematic diagram of the electronics system for the CsI(Tl) detector is depicted in Fig. 4. Every channel of the "raw" (CsI(Tl) + PMT) signal is amplified and shaped by the amplifier-shaper (AS), and subsequently digitized by the flash analog-to-digital convertor (FADC). The trigger system selects relevant events to be read out, while the logic control system provides a coherent timing and synchronization for the different electronics modules. The stability and linearity of the system is monitored (and corrected for, if necessary) by the calibration unit.

Two industry standards are adopted: NIM-convention for the AS and the various coincidence and veto logic modules, while the VME-protocols are used for the electronics-data acquisition interface. The trigger modules, logic control unit and calibration pulser are "double height" VME-6U modules, while the FADCs are "triple height" VME-9U modules. All are single-width modules.

The PMT signals pass through discriminators embedded in the AS module, and the NIM-level output are transferred to the trigger system. Simultaneously, the pre-trigger pedestals and the amplified AS pulses are continuously digitized and recorded on the circular buffers of the FADCs running at a 20 MHz (50 ns) rate. A typical FADC output signal of an event originated from the CsI(Tl) crystal is depicted in Fig. 2(b). The shaping effects can be seen when compared to the raw CsI(Tl) + PMT pulse in Fig. 2(a). The integrated area of the signal from two PMTs on the same crystal module added together gives the energy of the event.

The trigger logic depends on specific measurements. Once a signal due to a valid trigger is issued, the logic control system will generate a predefined "digitization gate" which determines the FADC digitalization time duration for the PMT signals. At the end of the gate, the FADC recording stops, and an "Interrupt" request is issued to the DAQ software hosted on a Linux-based PC via the VME-bus and a commercial VME-PCI bus bridge controller. The entire FADC system issues a single DAQ interrupt request (instead of each per module). The DAQ software responds accordingly, and the data from the FADC circular buffers are read out and saved on computer disks for further processing. A detailed description of the online and offline DAQ system is given in Section 4.

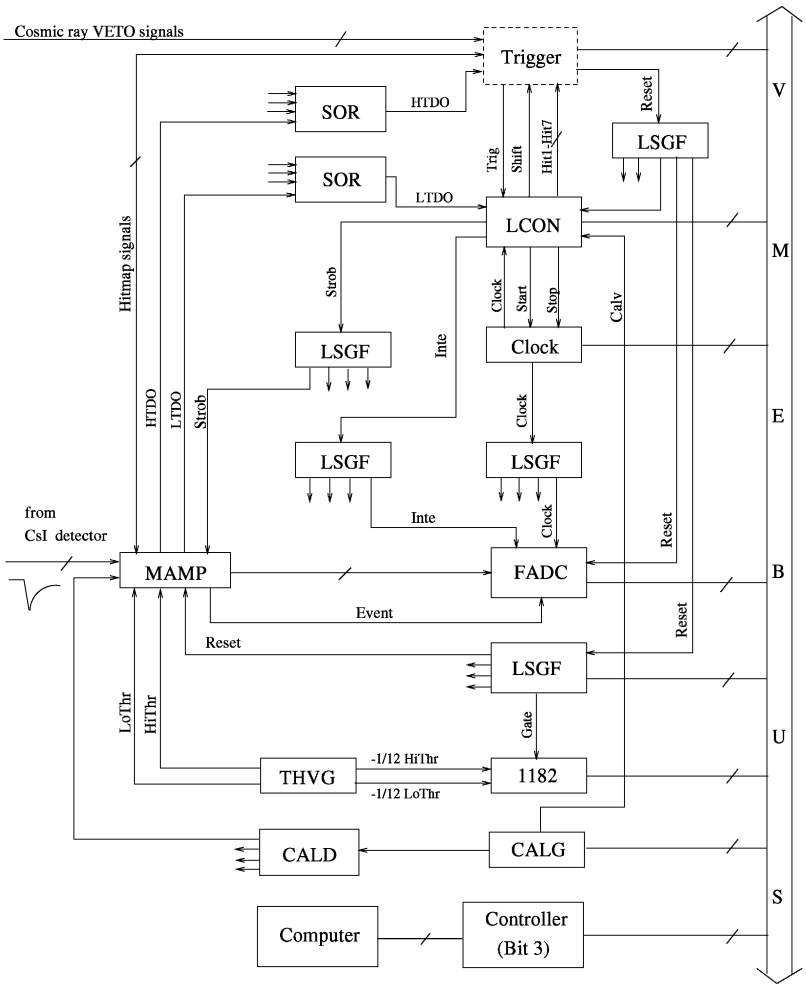

MAMP: Amplifier with 16-Channels ;
LCON: Logic Control Circuit ;
CALG: Calibration Signal Generator ;
CALD: Calibration Signal Distributor ;
THVG: Threshold Voltage Generator ;
FADC: Flash ADC ;
Clock: Clock circuit ;
LSGF: Logic Signal Fan-out ;
SOR: Signal OR ;
1182: LeCroy QDC

Fig. 4. A schematic diagram of the electronics system.

The calibration pulser generates and distributes simulated signals to monitor the functionalities and performances of all channels, helps trouble-shooting for locating noisy or dead channels and provides them with correction factors for subsequent analysis.

For optimal adaptations to our applications, as well as for cost-effectiveness reasons, almost the entire electronics and trigger system is designed, constructed, tested and made operational by the Collaboration.

The components of the electronics system are discussed in the following sub-sections.

3.1. Amplifier and shaper

The schematic diagram of the amplifier-shaper (AS) module is shown in Fig. 5. The AS receives

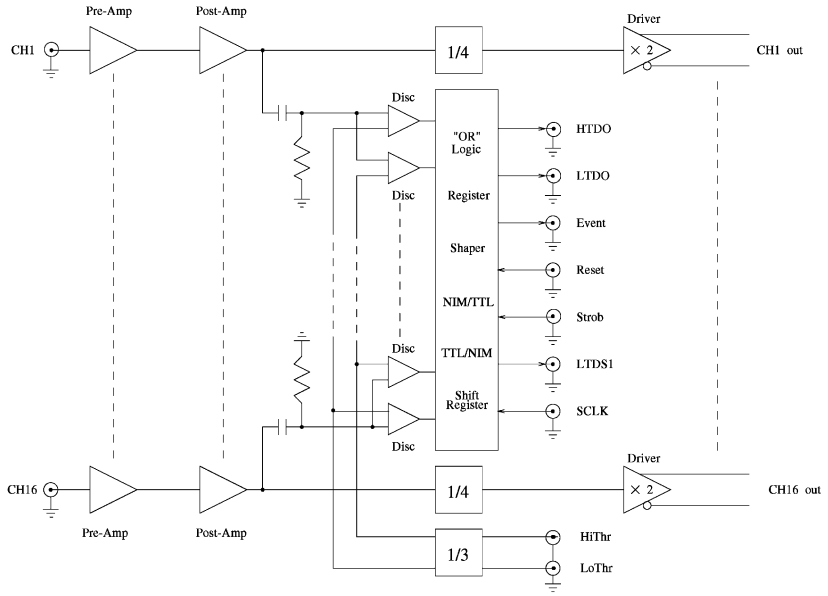

Fig. 5. A schematic diagram of the amplifier-shaper module, which contains 16 channels each with two discriminator outputs.

the PMT signals via LEMO cables and provides them with amplification, filtering, and pulse shaping. In addition, two discriminators per channels are integrated in the same module. A total of 16 channels are grouped into one module for the AS and the FADC.

The discriminator threshold levels for the PMT signals are provided by a separate manually set threshold voltage adjustment and distribution module. The high one (''HiThr'') is for trigger purposes while the low one (''LoThr'') allows recording of all signals just above electronics noise. The settings are constantly monitored by a commercial VME Charge-to-Digital Convertor (QDC) board.[4] The discriminator signals, ''HDTO'' and ''LDTO'' for those passing HiThr and LoThr, respectively, are sent to the trigger for processing by the trigger system.

As shown in Fig. 2(a), the raw signals originate as a summation of a collection of single photo-electrons (pe) statistically distributed over a time duration according to the standard light emission curve of the CsI(Tl). Therefore, they are several μs in length whose profile are rough with $\sim$10 ns spikes due to single pe. In comparison, thermal noise from PMT appear as the single pe spike with this $\sim$10 ns width.

The first stage[5] of the AS provides shaping at a time constant of 27 ns. It functions as a charge-sensitive amplifier for short (typically 10 ns and less) signals while remains as a current-sensitive amplifier for long (> 1 μs) signals. As a result, the single pe spikes are smoothened relative to the digitization time-bin of 50 ns, such that their amplitude are reduced to below the LoThr level. Consequently, the trigger threshold can be reduced, and the 20 MHz FADC clock rate is adequate. The subsequent stage[6] is a slow device providing effective shaping of about 250 ns and 1.6 μs in rise and fall times, respectively. The overall gain is 3.2 V/mA.

Each AS module is also equipped with a 16-bit shift register, which provides a hit pattern of the 16 channels on the module. The hit-pattern can be used to generate trigger decisions and to reduce the reading time of the FADC module. However, in a low count-rate experiment like ours, the DAQ

[4] LeCroy ADC 1182.

[5] Based on Harris IC HA-2525.

[6] Based on Analog Devices IC AD817.

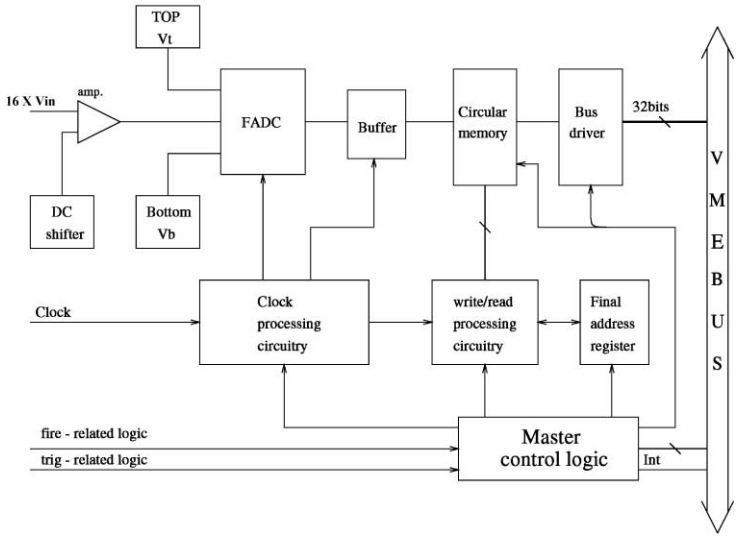

Fig. 6. A schematic diagram of the FADC circuitry. There are 16 channels in a module.

dead time is not of a critical concern, and therefore, this functionality of fast hit-pattern measurement is not implemented for the first operational version of the electronics system.

3.2. Flash ADC

The main tasks of the FADC are to digitize the pulse from the amplifier-shaper, and to issue an Interrupt request to the DAQ system. The schematic diagram of the FADC circuit is displayed in Fig. 6. There are 16 channels per module, matching the differential output signals from the AS delivered to the FADC with flat twisted cables. The resolution is 8-bit and the gain is adjusted such that the full dynamic range corresponds to an input of 2 V.

After an event is read out and the DAQ system is ready to receive the next event, a "Reset" signal is issued to the electronics hardware. The input signals (which are the AS output) are continuously digitized,[7] and the data are put into a circular buffer memory[8] of 4096 bytes (4 K in depth, with each bin having 8-bit resolution). The digitization frequency is driven by an externally programmable clock. The hardware limiting rate is 30 MHz, while typically a 20 MHz clock is used.

Digitization is terminated when the external clock stops at the end of a valid event: that is, typically 25 μs after a trigger is issued at "$t = 0$". All subsequent events up to a pre-selected time (typically 2 ms) are also recorded. The circular buffer points at the last byte it writes. The valid data on the circular buffer is then read out in the time-reversed sense, starting with the last byte until some pre-trigger time bins (typically 5 μs before $t = 0$) for extracting the pedestal information.

To enhance the reading speed, the 16 channels on one module are divided into four groups, and each group takes a 32-bit word for data transfer since the circular buffer for each channel uses 8-bit per recording. Based on special features to be described in details in Section 3.4, only those FADC modules with at least one hit above LoThr within the event duration will be read out.

3.3. Calibration pulser

The calibration pulser provides the information of dynamical range, linearity, and stability for all

[7] Based on Analog Devices IC AD775.
[8] Elite MT IC UM61256FK.

channels. It helps trouble-shooting to locate problematic channels, and provides a set of online or offline correction parameters.

As illustrated by the schematic diagram in Fig. 7, the pulser module consists of two components: calibration signal generator and distributor. The former generates a simulated signal, which is then fanned out via the latter to provide the input of the AS modules for all channels. A non-linearity of better than 0.3% has been achieved for all channels.

During steady-state data taking, the calibration will be performed several times in a day by the electronics system via fully automatic software.

3.4. Logic control unit

The schematic diagram of the logic control unit is depicted in Fig. 8. Its main function is to coordinate and synchronize the interactive actions of the various components of the electronics and DAQ systems. The corresponding timing schematics is shown in Fig. 9.

After receiving a valid trigger signal which defines the "START" time, control signals are distributed by the logic control unit to the various components. The hardware pre-selectable digitization gate, typically of 25 μs width, is initiated. At the end of the gate, a "STOP" signal is generated which disables the clocking circuit and the FADC digitization will stop.

For detailed diagnostics of the background events, it is desirable to record the possible occurrence of delayed correlated events, such as the ^{214}Bi–^{214}Po decay sequence mentioned in Section 2. Full digitization of the entire period far exceeds the available memory space in the circular buffer. To realize this requirement, a special "cascade-sequence" function is implemented after the completion of the triggered event, the entire system remains at the read-enable state capable of recording the pulse shape as well as timing of any delayed activities above LoThr for the duration of the "STROB" gate, typically set at 2 ms. Delayed events will initiate another cycle of digitization gate during which FADC digitization resumes, starting from the last location of the previous events. Relative arrival times of these delayed events are measured by additional Time-to-Digital-Convertors (TDCs) with 1 μs resolution. In this way, complete information up to 7 delayed events can be recorded (for a 20 MHz clock rate at the memory depth of 4 K). In addition, the computer time is read out for every event, providing complementary timing information between events. The measured timing uncertainty is close to the limiting accuracy provided by the resolution of 10 ms. Therefore, the detailed and complete timing sequence of all the events can be reconstructed offline, providing powerful diagnostic tools for background understanding and suppression.

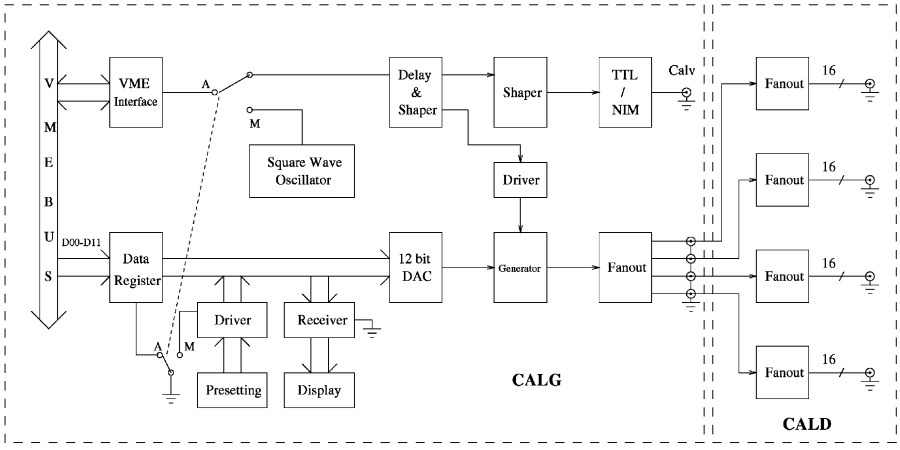

Fig. 7. A schematic diagram of the calibration pulser circuit.

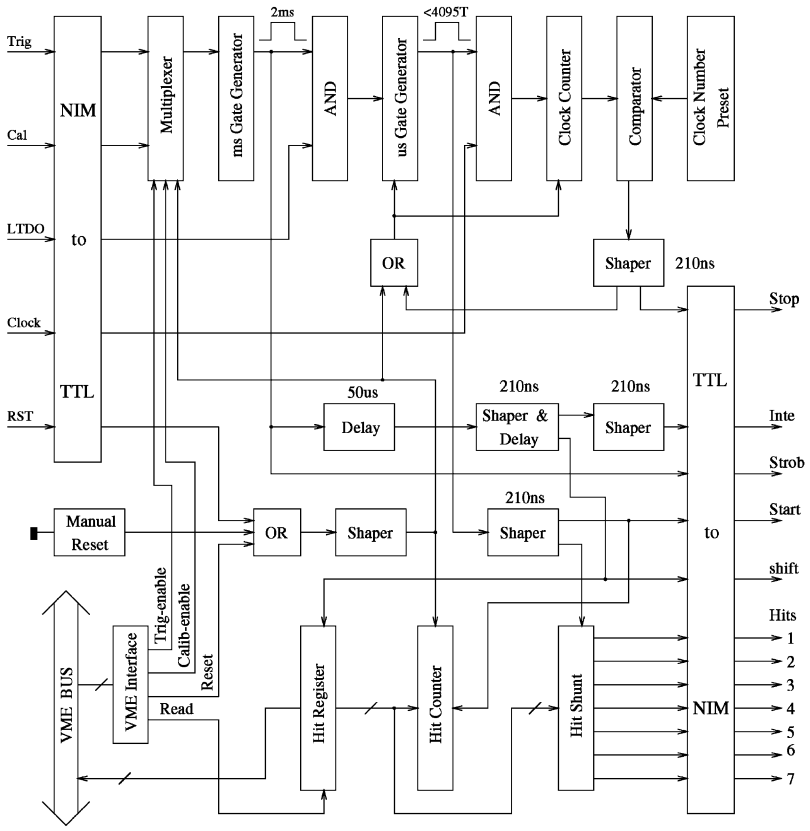

Fig. 8. A schematic diagram of the logic control unit.

A manual switch provides selection of data taking modes either with the cascade-sequence functionalities or in the single-event mode for calibration purposes.

An Interrupt (“INTE”) signal is issued to the DAQ system at the completion of the STROB gate. The DAQ system starts transferring the data from the FADC memory and other locations to the hard disk storage space in the computer. When data acquisition is successfully completed, a “RESET” signal is distributed to the entire system to turn it back to the read-enable state for the next event.

The INTE signal instructs the DAQ system to read out a valid event. For DAQ efficiency and data suppression reasons, only those FADC modules with valid data are read out. This is achieved when an “EVENT” signal is issued from an AS module via its respective FADC module to the DAQ system. This signifies that at least one channel has a data record above LoThr, and data will be read out from all 16 channels in this module. Software zero suppression is performed online and instantaneously on those channels without any signals above LoThr.

3.5. Trigger system

The trigger system is responsible for selecting events to be recorded. The schematic diagram is displayed in Fig. 10. A logic FAN-IN of the signals from all the cosmic veto scintillators, after a coincidence requirement within individual panels, generates the “V_{IN}” pulse. The veto action is extended over a hardware select-able “veto period”, typically of 100 μs, to get rid of background due to delayed cosmic-ray neutron-induced activities. The signal-definition line “S_{IN}” is

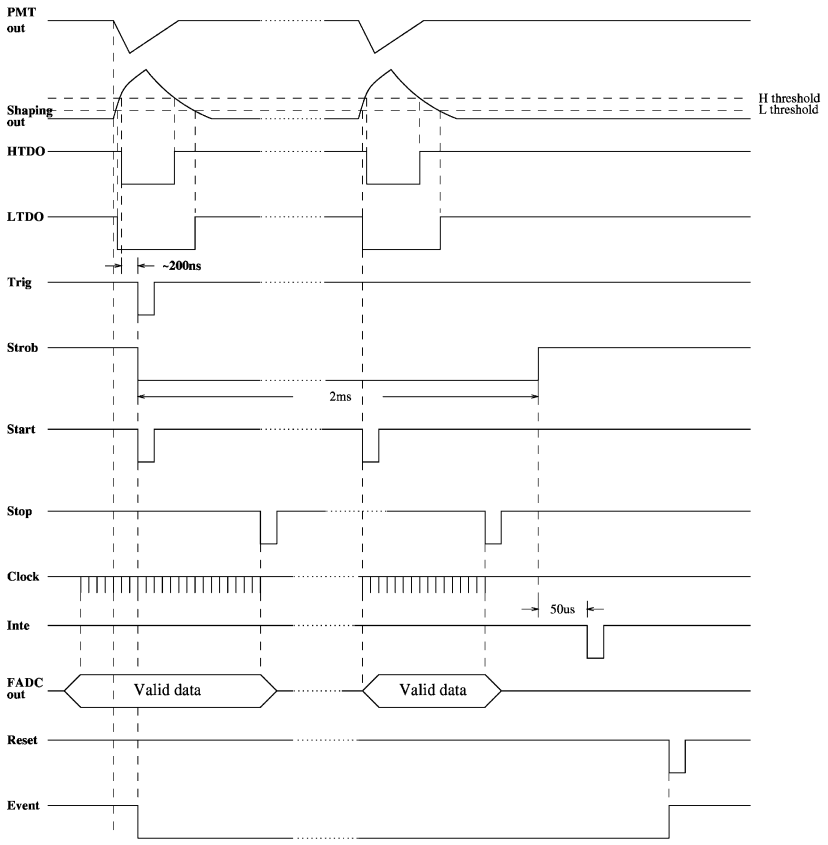

Fig. 9. The timing sequence in a typical event.

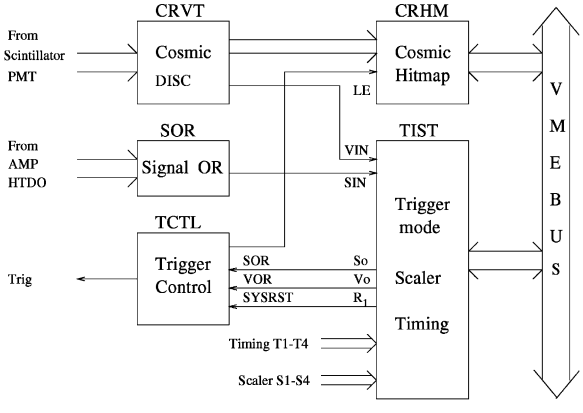

Fig. 10. A schematic diagram of the trigger system.

a logic FAN-IN from selected signals from the CsI(Tl) target.

Four software selectable trigger modes are implemented to serve various data taking purposes: $T1 = S_{IN}$, $T2 = V_{IN}$, $T3 = S_{IN} + V_{IN}$, and $T4 = S_{IN} + \bar{V}_{IN}$. The "physics trigger" is provided by T4, while T3 is used for dedicated data taking for cosmic rays, while T1 and T2 are for diagnostics and debugging purposes. In steady-state data taking, the "trigger menu" consists mainly of T4 with a small sample T3 and calibration pulser events taken once every several hours for monitoring and calibration purposes.

The definition of S_{IN} depends on the selection requirements based on the hit-pattern input from the various CsI(Tl) + PMT channels. For low count rate applications such as neutrino physics experiments, the trigger conditions can be kept loose and minimal, and can be fine-tuned to be optimized for specific physics focus.

The "minimal bias" trigger is a simple coincidence between the two PMTs corresponding to

the same crystal module, whose pulse height are above the HiThr discriminator level. This is realized by having the "left" PMTs connected to one AS module, and the "right" ones to another. A coincidence from the HDTO lines of these modules, followed by a logic FAN-IN circuitry provides the S_{IN} line. Detailed selection of signal events from the background (for instance, events with a single hit versus those with multiple hits) can be carried out with subsequent offline analysis.

The trigger system is equipped with other diagnostic tools, like hit-pattern units for the cosmic-rays veto panels, scalers for recording various count rates (like the trigger and veto rates), as well as TDCs for measuring various timing signals (like the time between the cascade sequence such as the one described in Section 2, as well as that between the S_{IN} and V_{IN} lines). The time between the most recent veto pulse and a valid trigger is recorded for diagnostic purposes.

4. Software system

The tasks of the software system are to perform data acquisition of the electronics discussed in Section 3, to operate a slow control system for the high voltage supplies and other ambient parameters, as well as to provide event display and monitoring graphic output. These functions are constructed in different programming languages and with different software tools, and work together in one PC running under the Linux operation system. Internet connection from the home-base laboratories (and indeed any external site) to the reactor plant is prohibited for security reasons. Accordingly, remote access and control to the reactor site can only be done with a telephone line dial-up solution.

The schematic framework of the software system, as well as the data flow, are depicted in Fig. 11. The FADC data are recorded on hard disks. Only minimal bias selection criteria are applied online. Event display for data-taking quality checks are provided for the on-site data taking.

At steady-state data-taking, the experiment is expected to be attended manually once per week. Filled-up hard disks will be replaced by new ones and brought back to the home-base laboratories where the data are copied onto CDs and Exabyte tapes for permanent storage. Meanwhile HBOOK [7] variable-array ("N-tuples") are prepared for the storage of refined data which passes some technical event filter criteria and contains useful reconstructed quantities, such as energy depositions and longitudinal positions, from the pulse shape information. The refinement process of raw data to N-tuples can be iterated as many times as needed based on better understanding on experimental running conditions and detector calibrations. The calibrated N-tuples are then distributed to collaborating laboratories for further physics analysis.

Unlike the electronics system where essentially all modules are designed and built by the Collaboration, the data acquisition and slow control systems are set up from commercially available hardware. Software codes, on the other hand, are developed and adapted to this specific experiment by the Collaboration.

Details of the various components are described below.

4.1. Data acquisition

The data acquisition (DAQ) system provides control to the experimental running parameters, accesses valid data from the VME electronics modules, and saves them on hard disks.

The host computer is a PC running with the Pentium III-500 processor using RedHat Linux as the Operation System. The PC masters the VME slave modules on both the 6U and 9U VME crates via a commercial adaptor system[9] which provides communication between the VME-bus and the PCI-bus.

The DAQ software can be divided into two components in kernel and user space. The program written at the Linux kernel space provides low-level access to the VME-PCI Adaptor, and serves as a device driver which uses the

[9] SBS Bit-3 Adaptor.

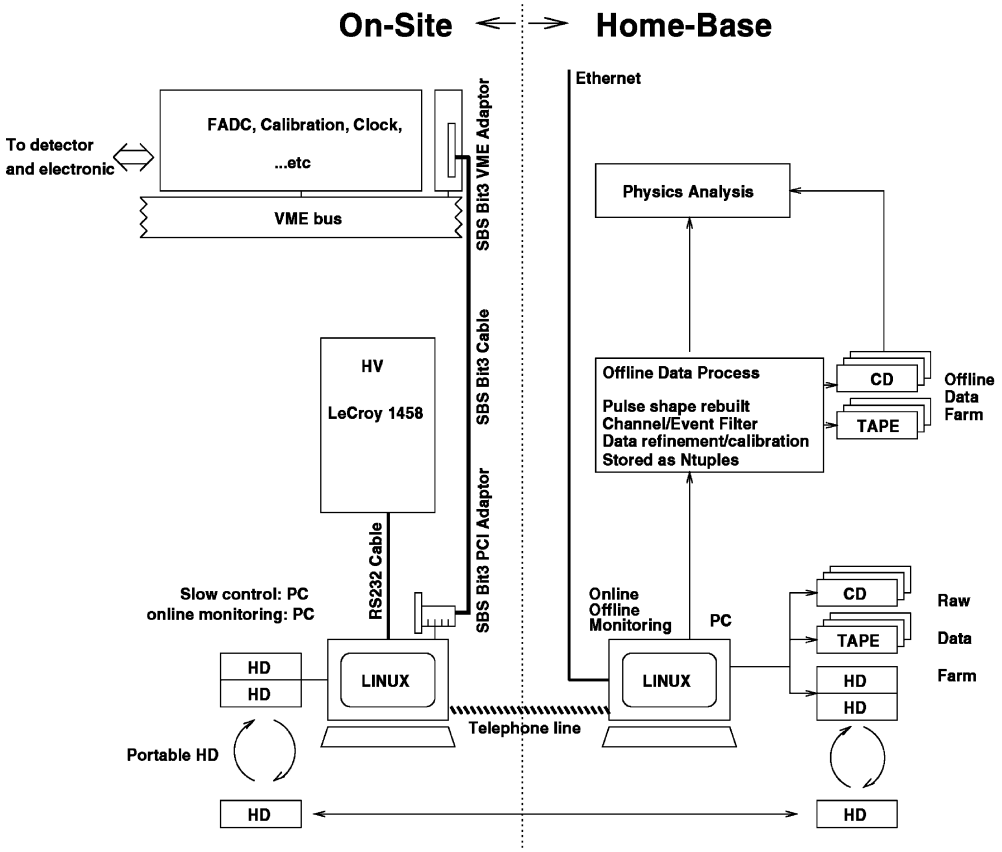

Fig. 11. A schematic diagram of the online and offline software architecture, indicating the data flow.

kernel functions and provides the entry-point where user-space programs can communicate with the hardware.

The Tk/TcL-based graphics user interface package is equipped with various operational dialogues, including the "Start–Pause–Stop" buttons and pull down menus for other functionalities for electronic module tests and regular DAQ operation. Various input fields are provided, where running conditions and parameters can be configured, file names and directory paths can be specified, and operational comments can be recorded. A function for pre-scheduling different trigger modes is also available which enables automatic selection of trigger conditions within the same data taking period. All control buttons in the dialogues are responded by their respective call-back functions at the kernel level of Linux.

4.2. Slow control

The slow control system serves to record and monitor the high voltage (HV) power supplies for the CsI(Tl) and veto scintillator PMTs, as well as other ambient and operation parameters.

The high voltage system is based on a dedicated main-frame crate[10] operating on special HV modules.[11] Each HV supply is distributed to two PMTs at the detector level. There are 12 HV supplies in each module and 16 modules can be

[10] LeCroy 1458.
[11] LeCroy 1461.

inserted into one crate, so that a crate can handle 384 channels altogether.

The crate is internally equipped with a micro processor, adequate RAM space, and communication ports which can receive and execute external commands or return the voltage and current status of the individual channels. The serial port communication are adopted (the other option is the Ethernet) via a RS-232C cable to the DAQ PC. In principle, one PC can host up to four serial ports with each port driving one crate, such that future expansion of the system is straightforward.

A VT100-based socket program is used to communicate with the PC serial ports using multiple Linux threads. Control and monitoring is achieved both locally on the console PC or remotely via the PPP (Point-to-Point Protocol) dial-up connection from home-base laboratories, as described in Section 4.4.

Slow control data such as output voltages and currents measured by the main-frame processor are recorded by the socket program on the hard disks of the DAQ PC, at a typical frequency of once per 10 min. Subsequent monitoring software packages can detect the voltage or current fluctuation, and warning or fatal error messages will be issued in case of alarms. Appropriate actions will be taken automatically, like voltage ramp-up for a tripped HV channel.

Other ambient conditions like temperature readings from thermostats, as well as operating parameters like the HiThr and LoThr values, are read out by a QDC module (see footnote 4). The cumulative count rates over a data-taking period from the CsI(Tl) target and the veto panels (the S_{IN} and V_{IN} lines, respectively) are measured by a scaler module.[12] Both are read out by the main DAQ program, at a typical frequency of once every hour.

The slow control functions consume very little CPU time, and therefore does not affect the DAQ speed, such that both operations can be handled by the PC without interference on the actual performance.

[12] CAEN V260.

4.3. Display and monitoring graphics

A PAW-based [8] event display and monitoring program enables data quality check on-site from the information provided by the pulse shape, energy spectra, hit map, and calibration pulser analysis. Both real-time and on-disk raw data can be accessed. The graphics panels paged with these specific functional buttons are implemented with PAW executable files, and can be linked together and switched between them on the HIGZ [9] window.

A clone of this program is duplicated on an off-site PC with an extra function which allows automatic data transfer (using a batch ftp shell script) from the on-site DAQ PC. To avoid the traffic caused by the low bandwidth of the networking telephone line, as discussed in Section 4.4, only a summary data in the format of HBOOK N-tuples and histograms are transferred back to home-base laboratories on a daily basis for offline monitoring and analysis.

4.4. Network connection

Owing to security reasons, the on-site computer can only be accessed via telephone line from home-base laboratories, as depicted in Fig. 11, to decouple the connections from the reactor plant's internal Ethernet network. The PPP system is adopted for the network connection of the on-site DAQ PC and the off-site PC, which serves the entry point for other off-site computers. Under the PPP client-server mode, the on-site PC is configured as the PPP server, whose modem can automatically pick up a dial-up connection request from the off-site PPP client, which gets its IP address from the server.

Both the server and client are equipped with 56k bit-per-second (bps) modems, and the bandwidth is limited by the quality (9.6k bps) of the existing internal telephone circuitry of the reactor plant. An average networking speed is around 4.8k bps is achieved. This is adequate for monitoring purposes when no large amount of data transfer is involved.

5. Performance

The electronics and data acquisition systems with a total of 200 readout channels has been operating under realistic conditions, taking data from the prototype crystal modules at the laboratory. The readout scheme essentially preserves all energy and timing information recorded by the detector, providing powerful diagnostic tools for rare-search type experiments.

Using the input from the precision calibration pulser, the overall linearity of the response of the electronics and data acquisition systems is better than 0.3%. The RMS of the pedestal is equivalent to 0.30 FADC-channel corresponding to 2.3 mV baseline noise at the input level of the FADC. The resolution of the measured pulser-charge as a function of pulse amplitude, in units of FADC-channel, is displayed in Fig. 12. The readout capabilities are much better than the detector response such that the overall performance parameters of the experiment are limited by the detector hardware.

The typical signals from the CsI(Tl) + PMT and the FADC outputs are displayed in Fig. 2(a) and 2(b), respectively. The fall times of the pulses are different between γ/e and α events, as shown in Fig. 13, providing a basis of particle identification. A typical cosmic-ray muon traversing a prototype detector set-up with seven crystal modules is presented in Fig. 14, demonstrating the time-synchronization among the different modules and channels.

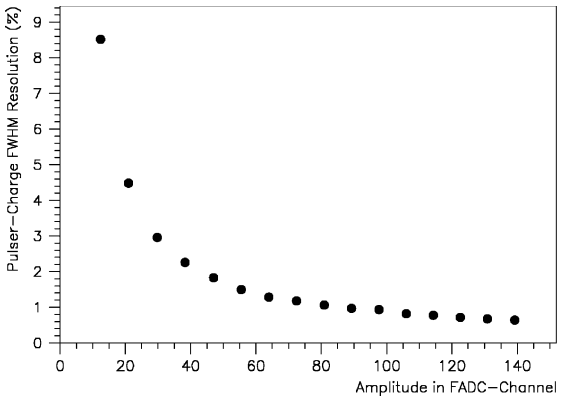

Fig. 12. The variation of FWHM resolution of the calibration pulser-charge as a function of pulse amplitude in units of FADC-channel. The full range of 255 corresponds to 2 V at the input level of the FADC.

The integrated sum of the PMT signals from the two ends of a crystal module gives the energy information of the event. A typical energy spectrum due to a ^{137}Cs source is depicted in Fig. 15. The integration time is 100 time-bin at 20 MHz, or 5 μs. An energy threshold of less than 50 keV is achieved. The full-width-half-max (FWHM) resolution at 660 keV is about 10%. This energy corresponds to pulses with amplitude of around 50 FADC-channels, which implies, as can be inferred from Fig. 12, a readout contribution of 1.6% to the resolution effects at the ^{137}Cs energy.

The system dead time is due to the contributions of two factors: (1) veto dead time, which is the veto rate multiplied by the inactive time per event (typically 100 μs), and (2) DAQ dead time, which is the time needed to read out the FADC and other modules (that is, the time after the STROB gate till the RESET pulse, as displayed in Fig. 9).

The DAQ dead time depends on the complexity of the events. To illustrate the range, the typical dead time is 16 ms to read out and zero-suppress the simplest event with single hit and without delayed cascade, requiring only one FADC per event to be handled. The corresponding dead time for the read-out of 9 FADCs each having Seven delayed cascades per event is 700–800 ms. Typically, in situations like calibration data taking with radioactive sources which give high count rate but simple hit-pattern, and where the delayed cascade functions are disabled, a DAQ rate of 100 Hz can be sustained.

6. Summary

An electronics and data acquisition system for low energy neutrino physics experiment, based on CsI(Tl) scintillating crystal as detectors with 100–500 readout channels, has been successfully designed, built and commissioned. It is modular by design and flexible in applications. One of the innovative features is the recording of the entire pulse shape and timing information up to the

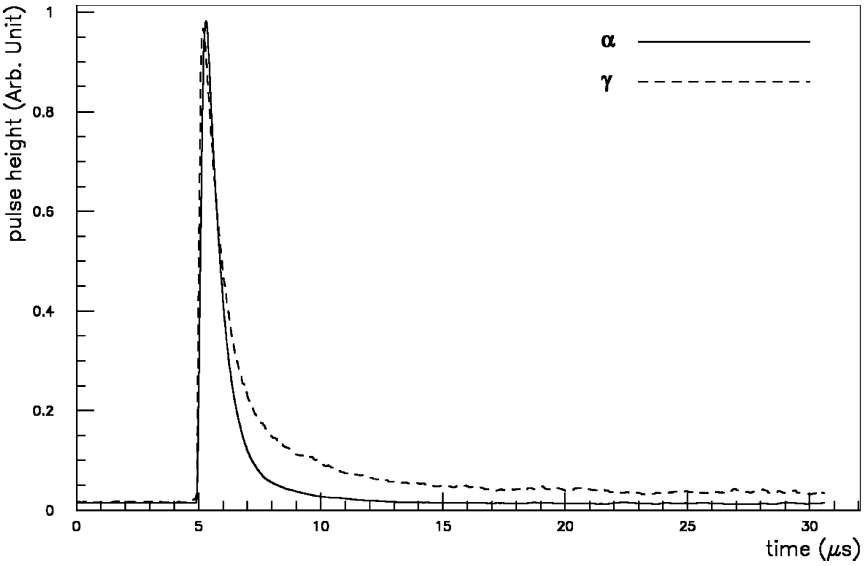

Fig. 13. The average pulse shape of events due to γ-rays and α-particles as recorded by the FADC module. The different decay times provide pulse shape discrimination capabilities.

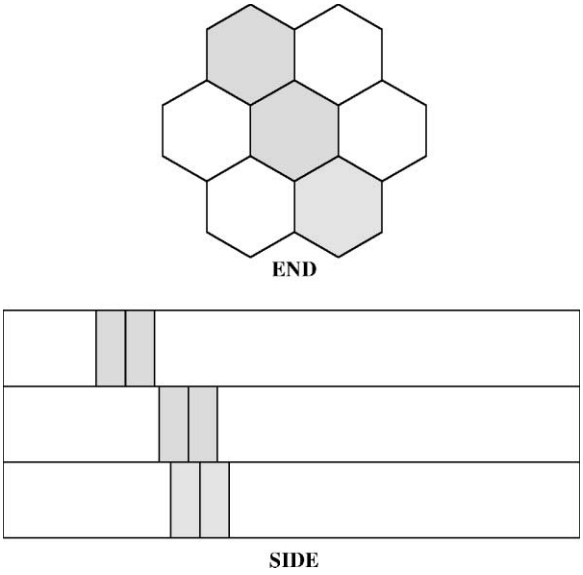

Fig. 14. A typical cosmic-muon event recorded by a 7-module/14-channel prototype detector, showing both the end and side views.

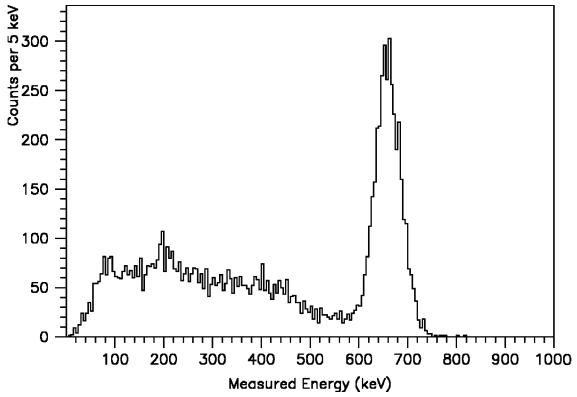

Fig. 15. The measured energy spectrum of a ^{137}Cs source. The FWHM resolution at 660 keV is about 10%.

range of several ms, providing powerful diagnostic tools to differentiate signals from background. The system can be adapted, as a whole or in parts, for other applications. For instance, the FADC module, together with the associated trigger and control electronics, have been used to read out signals from a high-purity germanium detector, retaining its very good energy resolution.

There are several possible future upgrades which can further enhance its capabilities. The amplifier/shaper modules are equipped with shift registers such that a hit-pattern can be extracted if necessary. The readout time can then be reduced with this prior knowledge of what channels to read. Similarly, the trigger conditions employed

for the current experiment are very loose and with minimal bias. With the exact hit-pattern information extracted, more sophisticated trigger selection criteria can be devised. Both functions are not critical for low count rate, low occupancy experiments, but may be desirable for higher trigger rate applications like in a high energy physics environment.

The current application requires a large dynamic range from about 10 keV (several photoelectrons from low-energy interactions) to 50 MeV (cosmic-ray muons). Although the FADC utilizes an 8-bit digitization scheme, its capabilities are beyond a $2^8 = 256$ fold dynamic range, since the entire pulse with a few hundred data-points is measured for every event. The energy is derived from the sum of hundreds of samples, each having an 8-bit range. An over-scale signal manifests itself as event with a "flat-top", the duration of which provides a measurement to the energy of the event. Using these features, the desired range can be covered even with a readout system having an 8-bit resolution in amplitude.

The authors are grateful to the technical staff of our institutes for invaluable support. This work was supported by contracts NSC 88-2112-M-001-007, NSC 89-2112-M-001-028 and NSC 89-2112-M-001-056 from the National Science Council, Taiwan, as well as 19975050 from the National Science Foundation, China.

References

[1] For the recent status on neutrino physics and astrophysics, see, for example, Y. Suzuki, Y. Totsuka (Eds.), Nucl. Phys. B Procs. Suppl. 77 (1999) 335.
[2] H.T. Wong, et al., Astropart. Phys. 14 (2000) 141.
[3] H.T. Wong, J. Li, Mod. Phys. Lett. A 15 (2000) 2011.
[4] H.B. Li et al., hep-ex/0001001, Nucl. Instr. Meth. A 459 (2000) 93.
[5] C.P. Chen et al., TEXONO Collaboration, Nucl. Instr. and Meth. A, submitted.
[6] P. Vogel, J. Engel, Phys. Rev. D 39 (1989) 3378.
[7] R. Brun et al., HBOOK-Statistical Analysis and Histogramming, CERN Program Library Long Write-Ups Y250, CERN, 1998.
[8] CN/ASD Group, PAW Users Guide, CERN Program Library W121, CERN, 1993.
[9] CN/ASD Group, HIGZ User's Guide and HPLOT User's Guide, CERN Program Library Long Write-Ups Q120 and Y251, CERN, 1995.